
This item was submitted to [Loughborough's Research Repository](#) by the author.
Items in Figshare are protected by copyright, with all rights reserved, unless otherwise indicated.

Experimental studies of the aerodynamics of spinning and stationary footballs

PLEASE CITE THE PUBLISHED VERSION

PUBLISHER

© IMechE / Professional Engineering Publishing

VERSION

VoR (Version of Record)

LICENCE

CC BY-NC-ND 4.0

REPOSITORY RECORD

Passmore, Martin A., Simon Tuplin, Adrian Spencer, and Roy Jones. 2009. "Experimental Studies of the Aerodynamics of Spinning and Stationary Footballs". figshare. <https://hdl.handle.net/2134/4610>.

This item was submitted to Loughborough's Institutional Repository (<https://dspace.lboro.ac.uk/>) by the author and is made available under the following Creative Commons Licence conditions.



For the full text of this licence, please go to:
<http://creativecommons.org/licenses/by-nc-nd/2.5/>

Experimental studies of the aerodynamics of spinning and stationary footballs

M A Passmore^{1*}, S Tuplin¹, A Spencer¹, and R Jones²

¹Department of Aeronautical and Automotive Engineering, Loughborough University, Loughborough, UK

²Wolfson School of Mechanical and Manufacturing Engineering, Loughborough University, Loughborough, UK

The manuscript was received on 8 March 2007 and was accepted after revision for publication on 18 September 2007.

DOI: 10.1243/09544062JMES655

Abstract: The accurate discrimination of the aerodynamic parameters affecting the flight of sports balls is essential in the product development process. Aerodynamic studies reported to date have been limited, primarily because of the inherent difficulty of making accurate measurements on a moving or spinning ball. Manufacturers therefore generally rely on field trials to determine ball performance, but the approach is time-consuming and subject to considerable variability.

The current paper describes the development of a method for mounting stationary and spinning footballs in a wind tunnel to enable accurate force data to be obtained. The technique is applied to a number of footballs with differing constructions and the results reported. Significant differences in performance are noted for both stationary and spinning balls and the importance of the ball orientation to the flow is highlighted. To put the aerodynamic data into context the results are applied in a flight model to predict the potential differences in the behaviour of each ball in the air. The aerodynamic differences are shown to have a considerable effect on the flight path and the effect of orientation is shown to be particularly significant when a ball is rotating slowly. Though the techniques reported here are applied to a football they are equally applicable to other ball types.

Keywords: aerodynamics, ball flight, lateral force, magnus force, footballs, spin ratio

1 INTRODUCTION

Sport is a global business and ball sports are the largest participating group. As major international companies strive for competitive advantage, methods enabling accurate discrimination of flight parameters are essential for product development. Sports governing bodies are also keen to control the performance of the balls for a number of reasons; to ensure consistency of performance in competition, to control the speed of the game, and in future, they may have an interest in controlling ball characteristics for safety and injury prevention. Aerodynamic studies reported

to date have been limited, primarily because of the inherent difficulty of making accurate measurements on a moving or spinning ball. Manufacturers therefore generally rely on field trials to determine ball performance, but the approach is both time-consuming and subject to considerable variability. Clearly, there is a need for a reliable method of measuring the subtle differences between ball configurations. A successful technique will aid in reducing product development time scales and provide the opportunity to tailor the performance of balls to suit the participants and spectators alike.

The work reported in the current paper concentrates on the development of a wind tunnel technique for obtaining accurate force data on stationary and spinning footballs. The technique is then applied to a number of footballs with differing constructions and the results reported. To put the aerodynamic data into context the results are then used in a flight

*Corresponding author: Department of Aeronautical and Automotive Engineering (AAE), Stewart Miller Building, West Park, Loughborough University, Ashby Road, Loughborough, Leicestershire LE11 3TU, UK. email: m.a.passmore@lboro.ac.uk

model to predict the behaviour of each ball in a number of typical scenarios. Though the techniques reported here are applied to a football they are equally applicable to most other ball types.

2 BACKGROUND

Aerodynamic effects play a crucial role in sports where the ball is given an initial impulse followed by a significant period of free flight. A well known example of this is a free kick during a game of football, but in practice the aerodynamic forces may be significant in any number of situations in the game. An aerodynamic force acts upon the ball during this free flight period, which can be broken down into a drag component in line with the direction of motion and an asymmetric force. The drag force comprises of two components, pressure and surface friction drag, with pressure drag the dominant mechanism. The asymmetric force acts perpendicular to both the direction of motion and the spin axis. It is caused by an imbalance of the pressure distribution around the ball and results in a deflection in the flight of the ball in the direction of the lowest pressure region. The non-uniform pressure distribution can result from several mechanisms, the most significant in football is generally considered to be the rotation of the ball that arises when the ball is struck off centre. The effect of the rotation is to advance the separation point on the counter rotating side, and to delay it on the opposite side. Asymmetric flow fields may also be generated by other mechanisms, for example, through differences in surface roughness on opposing sides of a non-spinning ball, however, such effects are generally only considered to be important in a few sports, for example cricket and baseball. By whatever means the asymmetric flow-field is produced, the lateral deflection is observed as swerve through the air, and it is the utilization of this that enables players to deceive the opposition. For the purpose of simplicity the asymmetric force is referred to as the lateral force throughout the current paper because the spin axis in the experiments and simulations is always vertical.

Throughout the last 30 years attempts have been made to replicate the flight of sports balls in laboratory conditions. Although many papers have been published on the testing of balls with zero spin, few have achieved controlled, repeatable measurements of the effects of spin on aerodynamic performance.

Experimental work by Achenbach [1–3] in the early 1970s established widely used benchmark data for the generic non-rotating sphere, defining the changing flow regimes with Reynolds number, the effects of surface roughness and vortex shedding patterns. The model used was 200 mm in diameter with a

polished aluminium surface which, for aerodynamic purposes, is considered smooth. The work was carried out in the Reynolds number range of 5×10^4 to 6×10^6 and therefore greatly exceeds the maximum Reynolds numbers seen in football where an upper ball speed of 45 m/s corresponds to a Reynolds number of approximately 7×10^5 .

Figure 1 illustrates a typical plot of drag coefficient against Reynolds number. In the subcritical region C_D is approximately independent of Reynolds number. In this regime the laminar separation, occurring at approximately 82° from the stagnation point [2], produces a large wake and consequent high drag coefficient. In the critical region the separation point moves rapidly downstream to approximately 120° with transition occurring first in the free shear layer associated with an intermediate separation bubble and then immediately without the formation of the bubble where the drag coefficient then reaches a minimum, for a smooth sphere, at a Reynolds number of approximately 4×10^5 . In the transcritical region following this the transition to turbulent flow occurs consistently at approximately 95° and the drag coefficient increases as the position of separation moves and the skin friction contribution varies. At Reynolds numbers above 1.5×10^6 an approximately constant C_D is again seen as transition moves to the forward part of the sphere. Achenbach [1] also investigated the effect of surface roughness using spheres with five different surface roughness values (the surface roughness was defined using k/d , where k was the roughness height and d the sphere diameter). It was observed that for increasing roughness the critical Reynolds number decreases, and both the minimum drag value and the trans-critical drag coefficient increase.

Experiments on rotating spheres are less widely reported. Lord Rayleigh [4] in his 1877 paper on the ‘irregular flight of a tennis ball’ acknowledged that

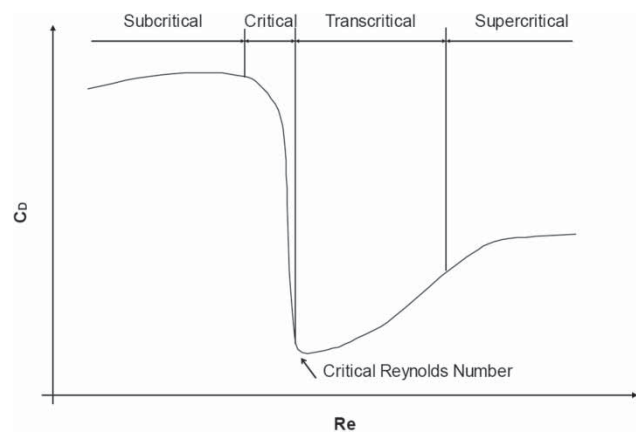


Fig. 1 Flow regimes of a smooth sphere (based on Achenbach [2])

the explanation of the effect had been correctly made by Magnus whose experimentation demonstrated that a rotating cylinder moved perpendicular to the onset airflow. The title 'Magnus effect' is now attributed to the phenomena of lateral force generation on rotating cylinders and spheres.

The practical testing of sports balls usually employs a wind tunnel, with the ball either mounted on a multi-axis force balance or with the ball introduced into the tunnel and allowed free flight. Davies [5] in 1949, introduced golf balls spinning up to 8000 r/min into a tunnel freestream by rolling them down an inclined plane. The longitudinal and lateral deflection was determined from where the ball struck waxed paper on the tunnel floor and with known initial conditions the aerodynamic loads were inferred using a flight model. Barton [6] used a similar test procedure for testing cricket balls, although they measured deflection using a stroboscope and photography. Briggs [7], used a rotating suction cup to apply the spin and then dropped baseballs into the tunnel. Bearman and Harvey [8] used a motor mounted within a model golf ball to impart the spin, with the model supported through wires attached to a balance. Rotational speed was measured using a stroboscope. Igor Sikorsky mounted baseballs on vertical slender spikes, driven by a motor mounted on the aerodynamic balance. He never reported the work himself, but Watts and Ferrer [9], repeated the work using a balance arrangement with the ball located through a single shaft. The ball was rotated in opposite directions to cancel the drag forces, with the resultant being the lift.

FIFA have clear guidelines for the manufacture, quality, and dynamic response of footballs [10]. The weight must be 410–450 g and the circumference 680–700 mm, there are also requirements regarding the dynamic behaviour but no standard for the aerodynamic response of the ball. However, the permissible variation in the diameter (216.45–222.82 mm) alone represents up to a 6 per cent change in the projected area of the ball and hence for two otherwise aerodynamically identical balls a potential 6 per cent difference in aerodynamic load.

In addition, there are a number of other factors that may influence the aerodynamic performance that are not covered by the regulations. These include seam consistency and depth, panel configuration, surface material (type and wear), orientation of the valve, and sphericity. Gaining an understanding of the influence of these parameters would allow the future manufacture of footballs with a known and consistent aerodynamic response.

There is little published data specifically on football aerodynamics. An article published by PhysicsWeb [11] gives an estimate of the critical Reynolds

number to be at approximately 4×10^5 , and quotes a Magnus force of 3.5 N for 10 r/s and 30 m/s, but does not indicate where this data came from or how it was obtained. Indirect force estimations have been made by Carre *et al.* [12], who fired footballs from a specially designed projection machine and recorded the flight using two high speed cameras. The forces were calculated using a flight model and optimization code, assuming that C_D , C_L , and spin rate were constant throughout flight. C_D was, however, found to vary with launch velocity throwing some doubt on the initial assumptions. Comparison with results from Achenbach [1] indicate that a football behaves like a 'slightly rough sphere', (estimate $k/d = 60e^{-5}$). In a further study Carre *et al.* [13] tested a one-third scale rapid prototype and a miniature football in a small wind tunnel and reports both static and spinning tests. Figure 2 shows coefficient data from the literature including different ball types and smooth sphere results.

3 EXPERIMENTAL SETUP

The open circuit wind tunnel has a closed working section of 1.32×1.9 m giving an approximate blockage ratio of 1.70 per cent for a football. The maximum working speed of 45 m/s is well above the maximum of 34 m/s reported by Neilson and Jones [14] for a free kick and gives an upper Reynolds numbers of $Re_{max} = 6.8 \times 10^5$ based on ball diameter. The working section turbulence intensity is approximately 0.2 per cent and spatial uniformity ± 0.2 per cent of mean velocity. For further details on the tunnel, see Johl *et al.* [15].

The aerodynamic balance is a high accuracy six-axis under-floor virtual centre balance designed for aeronautical and automotive testing. The quoted accuracy for the relevant balance components is ± 0.012 N for drag and ± 0.021 N for side force and using an estimate of the expected forces from a football at maximum spin rate and tunnel speed, the resolution obtainable is; ± 0.05 per cent of full scale for drag and ± 0.50 per cent full scale for the lateral component.

The ball spin apparatus is shown mounted on the balance under the tunnel working section in Fig. 3(a). For purposes of scale, each of the four supporting legs has a 50 mm square cross-section. The structure supports a bearing casing and motor driving a 20 mm diameter (circular) shaft that protrudes through the tunnel floor. Figure 3(b) shows the ball mounted on the shaft and in the wind tunnel working section.

Mounting the ball from a single shaft from below was considered the best option for minimising the flow interference whilst maintaining a simple

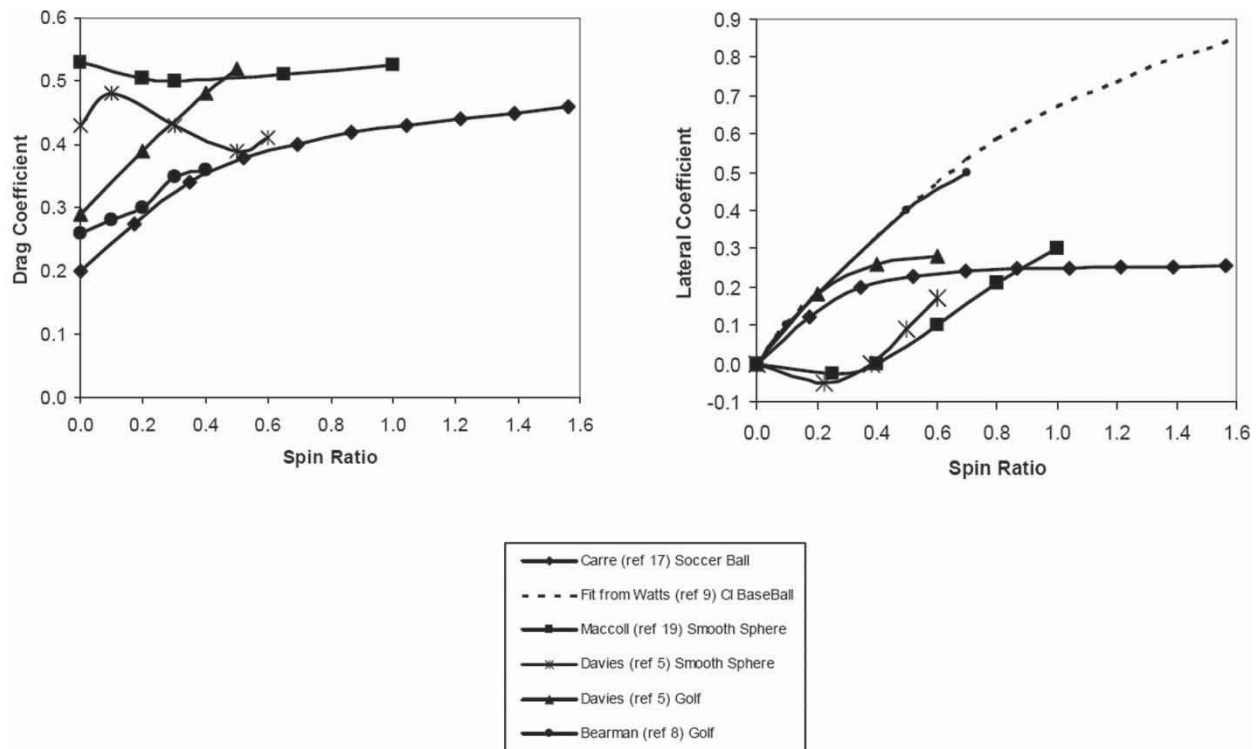


Fig. 2 Summary of published spinning ball data

design. A shaft diameter of 20 mm ensures that the shaft does not deflect significantly under load whilst being less than the recommended 10 per cent of the ball diameter [2, 9]. The motor has a maximum rated speed of 4500 r/min, well in excess of the maximum recorded spin rate of a football from a free kick of 866 r/min recorded by Neilson and Jones [14], but this makes the rig suitable for other ball types where the spin rates are much higher.

To provide secure mounting on the shaft, the real footballs are filled with a two-part poly-urethane expandable foam which is then drilled to accommodate the shaft. Minimizing mass imbalance of the

test ball was also considered critical to obtaining aerodynamic force measurements uncontaminated by dynamic forces generated by the motion of the ball and support. Careful preparation of the test ball was done to facilitate this. First, the injection point of the foam was through a hole generated by drilling out the inflation valve, thus the only obvious mass imbalance was removed. An 8 mm outside diameter (OD) steel tube was inserted through this hole to allow the air to escape during the expansion of the foam. The ball is then placed into a two-part spherical mould with the tube protruding through the top of the mould, and the mould closed. The foam is injected in through the tube during its cream stage (lasting for 30 s after mixing until expansion occurs) which ensures that the foam goes immediately to the bottom of the ball, thus rising upwards and expelling excess air out of the top. The ball is then left to cure for 24 h and a homogeneous foam density is achieved within the ball. This process has the added advantages that the real footballs tested here all have the same diameter (215 mm), while also ensuring sphericity.

Several methods of locating the ball on the support shaft were tried. The most successful method was to mount the ball in a lathe and bore an 18 mm hole through the centre with a sharpened tube. The splined support shaft was then pressed into the hole and bonded in place. The balance of the ball was tested by monitoring the vibration at the bearing

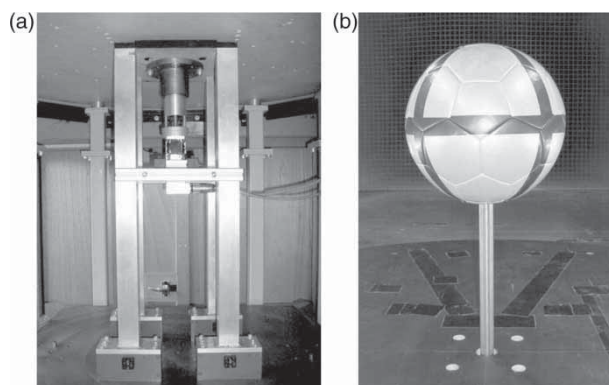


Fig. 3 Experimental setup (a) under-floor view and (b) ball *in situ*

housing with a vibrometer. Wind off data recorded from the balance with the ball spinning resulted in no forces being recorded within the repeatability of the balance ($\pm 0.1\text{N}$).

Two rapid prototype full size models (balls 1 and 2) and four real footballs (balls 3 to 6) were tested and are summarized in Fig. 4. Ball 1 has a smooth surface finished by hand. Ball 2 has a similarly smooth finish, with 32 panels in a regular arrangement of 12 hexagons and 20 pentagons. Balls 3 and 4 have the same panel arrangement as ball 2 with ball 3 having a conventional surface finish and ball 4 having regularly spaced dimples 4 mm in diameter and 0.5 mm deep. Ball 5 has a similar panel arrangement but the 12 hexagons are joined to create six 10 sided panels. Ball 6 has a tessellation of the four panels seen in the figure with a total of 24 panels. In addition, ball 3 is a bonded construction and balls 4, 5, and 6 are conventional stitched constructions. All balls were mounted through and perpendicular to the valve. The illustrations in Fig. 4 are the view taken from directly above the ball. The bottom of each illustration is the upstream side of the ball at zero yaw.

In both static and rotating cases balance samples were taken over a 20 s period at a sample rate of 5 Hz to remove any unsteady effects. The balance software internally averages the forces and records the mean value. The support interference effect, measured in a separate test (with the ball mounted in its usual location but independently of the support) was then subtracted to yield the ball forces. The support interference drag is 2.3 N at 30 m/s, which is approximately 20 per cent of the total drag force. In the calculation of coefficients the reference area is the projected frontal area of the specific ball

under test, calculated from the mean ball diameter. The latter was obtained from the mould used during the ball preparation.

During rig commissioning, the effect of the motor power cable and rig vibration were shown to have no significant effect on the mean forces recorded but from direct measurement of the rig vibration it was concluded that the maximum spin rate should not exceed 600 r/min. During commissioning, repeatability tests showed a maximum scatter of approximately $\pm 0.1\text{N}$ on both drag and lateral force at the 95 per cent confidence level. This translates to an error in the drag and lateral force coefficients of ± 0.04 at 10 m/s, ± 0.009 at 20 m/s, and ± 0.005 at 30 m/s.

4 RESULTS

4.1 Stationary tests

Figure 5 shows the Reynolds sweep for ball 3 along with other published results for non-rotating spheres and balls.

Below transition, C_D is approximately 10 per cent higher than that of a smooth sphere. The additional drag may be produced by higher skin friction and possibly as a consequence of small local separations caused by the ball seams. Alternatively, it may be associated with the support from below, this is essential to produce high quality spin results but is a compromise over the more usual support from behind through the wake. Transition occurs at a Reynolds number between that of the smooth and uniformly rough sphere at a speed of approximately 15 m/s. This speed is well within the normal operating range for a football during a match. The supercritical C_D is comparable with that of the rough sphere.

A number of authors have reported changes in aerodynamic coefficients with orientation of the seam and in many sports such variation is knowingly exploited to good effect. Alam *et al.* [16] indicates that seam orientation of tennis balls is found to have an effect on C_D at low Reynolds numbers, but no indication of the size of the variation is given. Watts and Sawyer [17] found, in wind tunnel tests of non-rotating baseballs, that seam orientation had a significant effect on both C_D and C_L for a baseball tested at 21 m/s. It was concluded that the largest changes of lateral force coincided with the seams being in the approximate position of the separation point. Large fluctuations in force were also seen, and were attributed to the separation point moving between the front and the back of the seam.

Figure 6 shows the drag coefficient and lateral force coefficient for the two rapid prototype cases. This comparison provides the opportunity to isolate the

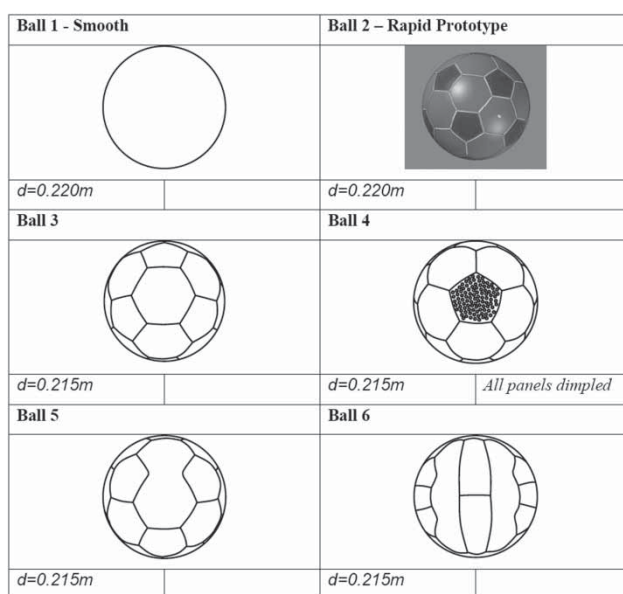


Fig. 4 Ball configurations

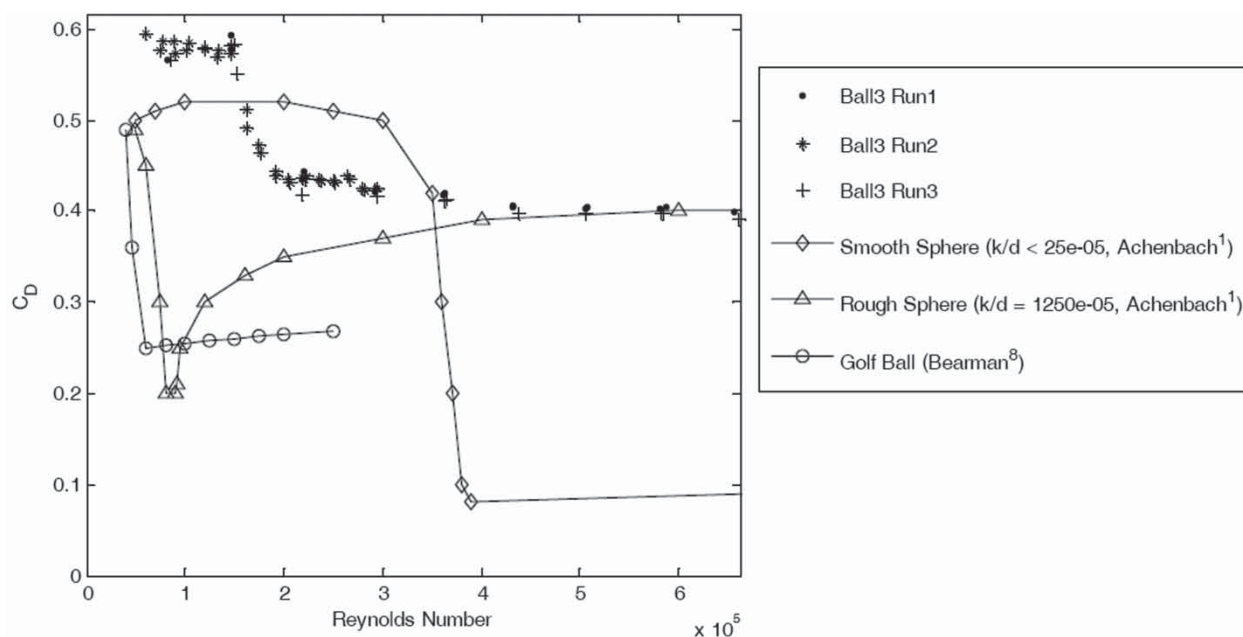


Fig. 5 Non-rotating ball drag coefficient against Reynolds number

effect of seam orientation without the potential problem of sphericity that may arise in comparing two real balls.

For ball 1 (smooth ball) the variation seen in both coefficients is within the stated coefficient uncertainty of ± 0.005 . The slight trend seen in the results is thought to arise from the practical setup of the ball in the tunnel and its mounting on the support sting. The variation that arises with the model football (ball 2) is, however, significant and implies that a non-rotating ball may swerve in flight, though not to a predictable degree and may go to the left or right. It may also be concluded that for a very slowly rotating ball the degree of swerve may vary

throughout its flight. Such results have not been reported before for this type of ball. Carre *et al.* [13], in experiments with footballs, concluded that there are no effects on C_D due to ball orientation, but in that work the rotation of the ball was about the streamwise axis and could not therefore be expected to have an effect.

Figure 7 shows the effect of orientation for the four real footballs. In all cases a similar response to that of the rapid prototype is seen though the magnitude of the coefficients is generally greater. Ball 6 demonstrates the largest lateral coefficients of approximately 0.15. This represents a lateral force in excess of 3.0 N at 30 m/s. Such variation is assumed to arise as the separation line moves with the seams and, with such complex seam patterns, the separation may be quite different on the two sides of the ball. This gives an asymmetric flow field and hence lateral forces and, where the seam moves the separation point upstream, increased drag. A better understanding of the mechanisms at work here can only be gained through detailed flow field measurements, but may lead to improved future designs.

To more accurately quantify the variation seen in Fig. 7 the standard deviation for all six cases have been calculated and are presented in Table 1.

Ball 6 shows the largest variation and, in addition to the difference in panel arrangement, it was noted that each panel appeared to take a separate form rather than being truly part of a continuous sphere. It is possible that this promotes larger local separations in some orientations, increasing the ball sensitivity. Balls 3 and 4 have the same panel arrangement as the rapid prototype ball 2 but both show some

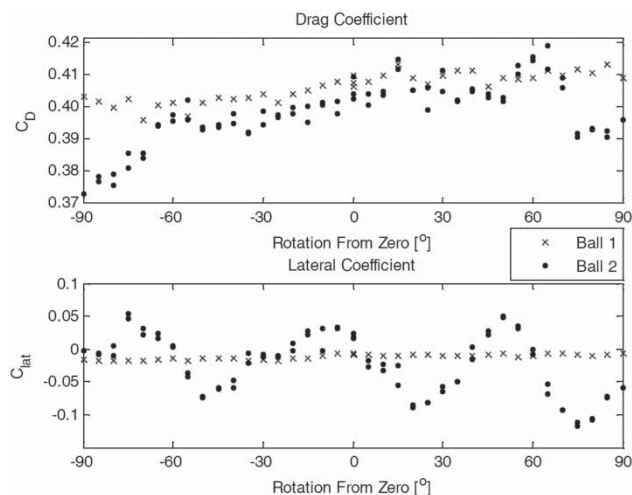


Fig. 6 Effect of orientation on aerodynamic coefficients – rapid prototypes. $Re = 4.5 \times 10^5$

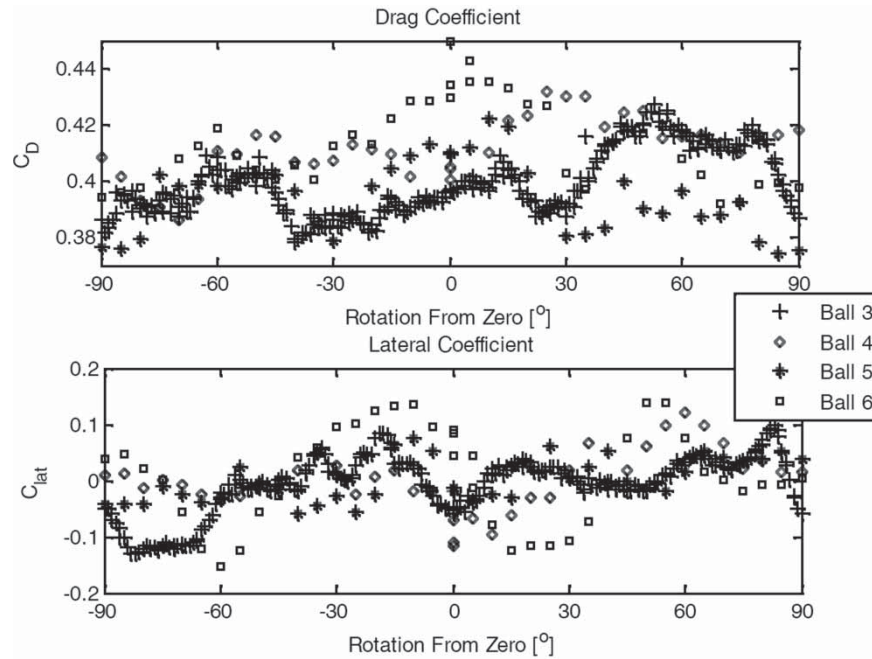


Fig. 7 Effect of orientation on aerodynamic coefficients – real footballs

increased variation over it. The dimples on ball 4 do not appear to have an effect on lateral force generation, but there is a small reduction in the variation in drag. The least sensitive ball regarding lateral force is ball 5, which can be simply attributed to the reduction in seam numbers.

4.2 Rotating tests

The spin tests were limited to the real footballs because the rapid prototype models were more prone to out of balance forces because of the internal structure formed during the manufacture. Each ball has been tested between 0 and 600 r/min in 100 r/min steps and from 10 to 30 m/s in 10 m/s steps. For ball 3 the tests were conducted at 50 r/min intervals. These spin rates and speeds do not cover the complete range reported in some literature but the results suggest that they cover most of what is practical during a football match.

Table 1 Standard deviation in static aerodynamic coefficients

Ball number	Standard deviation in C_D	Standard deviation in C_{LAT}
1	0.0044	0.0041
2	0.0097	0.0450
3	0.0117	0.0527
4	0.0110	0.0530
5	0.0130	0.0386
6	0.0151	0.0858

Figure 8 shows the drag and lateral coefficients for ball 3 plotted against non-dimensional spin parameter ($\omega r/U$). Measurements were taken through increasing and decreasing spin rates but it is evident that there is little or no hysteresis. The dependency on Reynolds number is seen to reduce for the drag above the critical value but a similar trend is not seen for the lateral force over the Reynolds number range tested. Both Smits [18] and Bearman and Harvey [8], in their work on golf balls reported a similar result for C_D but also showed a reduction in Reynolds number dependency for the lateral coefficient.

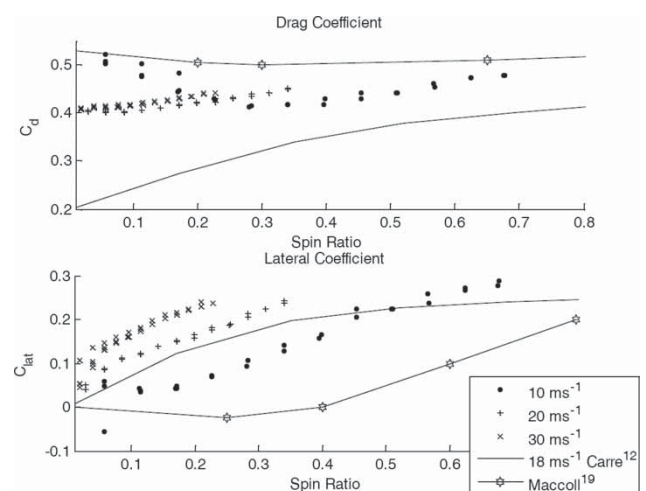


Fig. 8 Ball 3 aerodynamic coefficients as a function of spin ratio

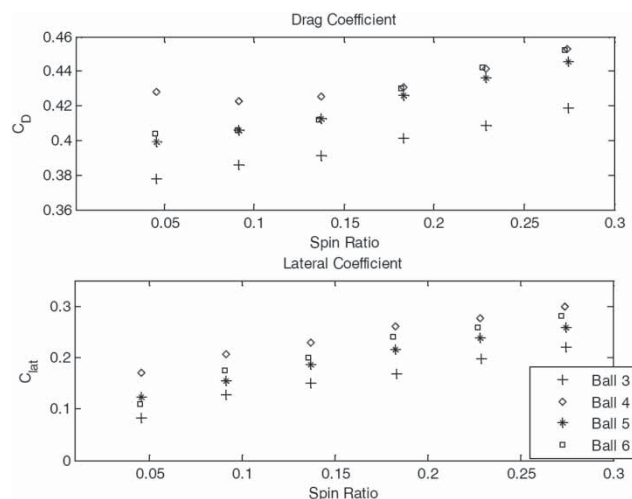


Fig. 9 Comparison of aerodynamic coefficients as a function of spin ratio for four ball types

As both C_D and C_L are Reynolds number and spin rate dependent and both velocity and spin rate will decay during flight all of these effects should be included in any flight model. This may explain the low C_L and very low C_D values reported by Carre *et al.* [12] who assumed these as constants in the flight model used for determining the coefficients. The results of Maccoll [19], also included in Fig. 8, were obtained on a wooden sphere at a Reynolds number of 1×10^5 .

Figure 9 shows a direct comparison of force coefficients of balls 3 through 6 over the spin ratio range at a tunnel speed of 30 m/s.

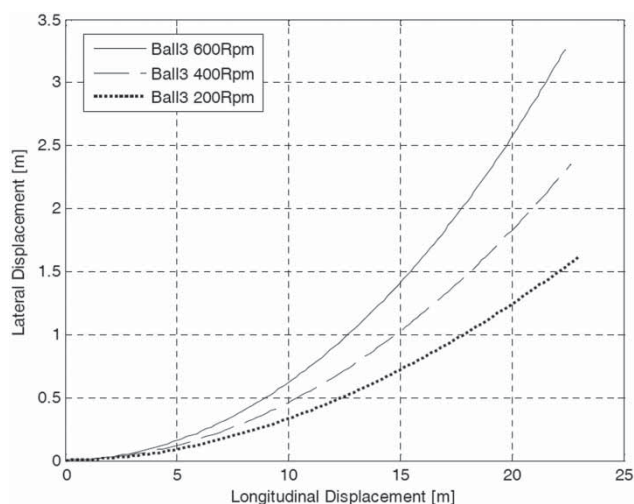


Fig. 11 Effect of ball spin rate on lateral deflection, flight model prediction

Significant differences in the actual values of both the drag and lateral coefficients are seen for the different ball constructions, but for drag and lateral coefficients the dependence on spin ratio is consistent for all but the drag on ball 4. Ball 4 has the dimpled surface finish and appears to exhibit a minimum drag coefficient at a spin ratio of approximately 0.1. The differences seen in the ball constructions are significant from an aerodynamic perspective but whether they are sufficient to produce a practical difference in a game situation requires some flight predictions based on the aerodynamic data.

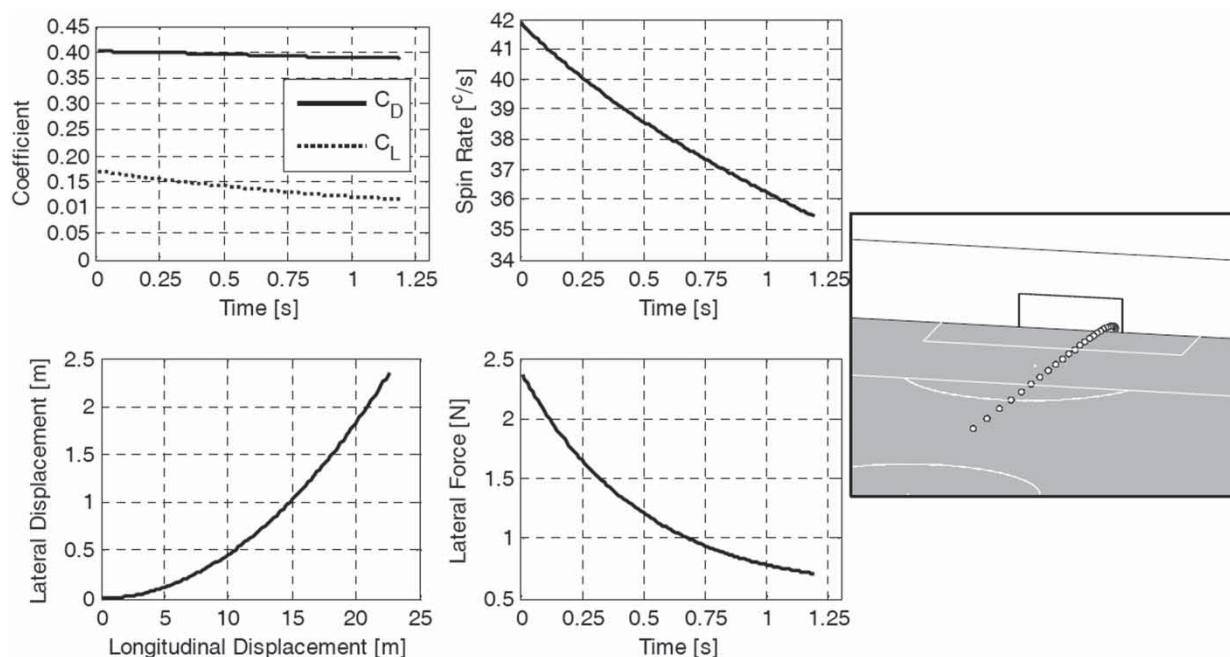


Fig. 10 Example ball flight model output

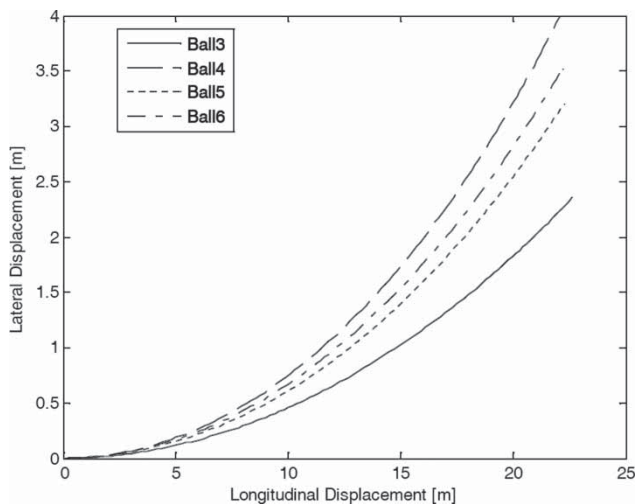


Fig. 12 Comparison of ball construction type on lateral deflection, flight model prediction

4.3 Effect of aerodynamic parameters on flight

The flight model is based on that reported by Bray and Kerwin [20] with the spin axis assumed vertical and a look up table of drag and lateral force coefficients. In addition, a crude model of spin decay based on flat plate skin friction is implemented. This models the ball as two flat plates, each of half the ball surface area, and then uses the mean tangential velocity for each of the two sides of the ball to calculate the skin friction. The spin degradation model and the collection of spin degradation experimental data is the subject of future work. The flight model is implemented using first-order backward differencing, where the time step has been reduced until there is no significant difference in the final ball position.

An example simulation is shown in Fig. 10 for a free kick taken using ball 3 with an initial velocity of 30 m/s, spin rate of 400 r/min about the vertical axis and a launch angle of $\theta = 15^\circ$ from the horizontal.

The continuous arc of the flight demonstrated in this figure contradicts the impression sometimes stated that some players have the ability to make balls swerve late in the flight. A much more sensible explanation, which agrees with the results presented here, is given by Craig [21], who suggests that because the human visual system is poorly adapted to accelerated motion, the ever varying degree and direction of acceleration caused by a spinning ball cannot be anticipated well. However, it is also important to note that in this simulation the ball does not pass through transition and in this region it is possible that some different effects might be encountered.

The influence of spin on the ball is shown in Fig. 11 which shows the paths of the ball for 200, 400, and 600 r/min, all with an initial velocity of 30 m/s.

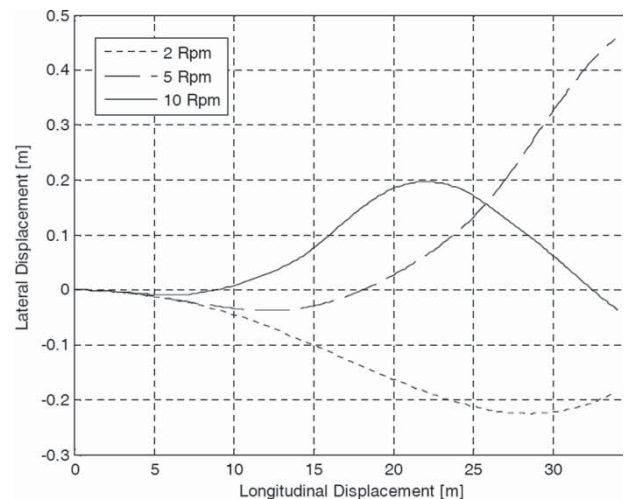


Fig. 13 Flight path for a slowly rotating ball, quasi-static flight model prediction

A strike from the edge of the penalty area (18 yards) laterally deflects by about twice as much, when the spin rate is increased from 200 to 600 r/min.

The effect of ball construction is shown Fig. 12 where each of the four real footballs tested has been subject to the same initial conditions of 30 m/s and 400 r/min spin about the vertical axis. For the example used in the previous case of a shot from the edge of the penalty area the balls would laterally deflect by approximately 1.35, 2.0, 1.8, and 2.25 m (balls 3, 4, 5, 6).

During the wind tunnel tests the considerable effect of ball orientation was explored. Using this data within the flight model and assuming quasi-steady conditions, the flight of ball 3 at low rotational speeds and with an initial translational velocity of 30 m/s is predicted. The results are shown in Fig. 13.

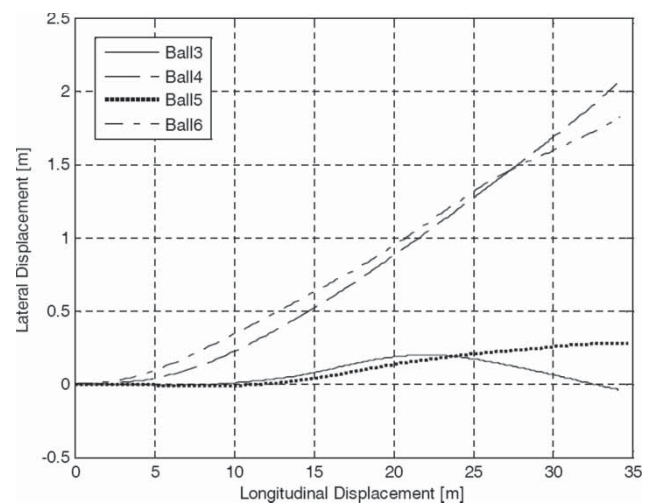


Fig. 14 Predicted flight path of real footballs rotating at 10 r/min

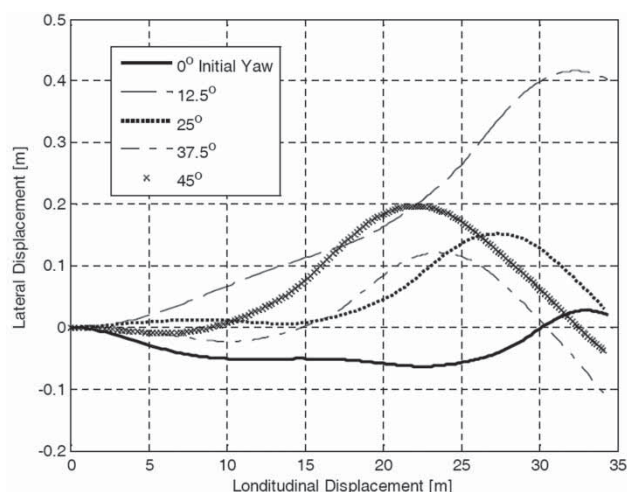


Fig. 15 Predicted effect of initial orientation on flight path of a slowly rotating ball

When the ball rotates slowly, the lateral force varies dramatically (Fig. 7(b)). Under these conditions the path no longer has a consistent curvature and is particularly sensitive to quite small differences in the spin rate. It is suggested that it is this behaviour that can lead to potential complaints regarding the performance of a particular ball. Figure 14 shows all four balls with a spin of 10 r/min and further reinforces this conclusion as the four different ball types behave quite differently.

Balls 4 and 6 simply appear not to fly in a straight line, diverging by about a metre in 20 m. Balls 3 and 5 travel much more closely to the intended direction but may be perceived as being unsteady in flight.

In both Figs 13 and 14 the initial condition for each ball is the zero degree orientation used in the wind tunnel tests. In practice this is simply a convenient reference point and the initial orientation will also have an influence on the path of the ball. Figure 15 shows the path travelled by ball 3 for a range of initial conditions. The differences are relatively small but may in some circumstances be sufficient to deceive the opposition. It is also possible that some players are aware of these differences and therefore place the ball for free kicks in a particular orientation to ensure consistent flight.

5 CONCLUSIONS

1. A technique for accurately measuring the aerodynamic loads on stationary and rotating balls has been developed. The technique has been proven on footballs but is equally applicable to other ball types.

2. The accuracy of measurement of aerodynamic loads is approximately $\pm 0.1\text{N}$ on both drag and lateral force at the 95 per cent confidence level. The accuracy of the coefficients is dependent on wind speed and is approximately ± 0.04 at 10 m/s, ± 0.009 at 20 m/s and ± 0.005 at 30 m/s. Repeatability tests confirm this.
3. The results demonstrate that the facility can be used to discriminate between ball types and in assessing the effect of seam orientation.
4. The subcritical C_D of a real football (3) was found to be around 10 per cent higher than a smooth sphere. Transition occurs at a Reynolds number of 1.5×10^5 , approximately half way between that for a smooth and a uniformly rough sphere.
5. In non-rotating testing the orientation of the balls has a significant effect on the drag coefficient and considerable lateral forces are also produced in some orientations.
6. Using a flight model to predict the ball path, the lateral forces measured in non-rotating tests are shown to have a considerable effect on the directional performance of the ball during flight. This may be seen by players as the ball simply swerving during flight, or being somewhat unstable.
7. In tests on a single spinning ball the drag coefficient is shown to become independent of Reynolds number above the critical value, however, this is not the case for lateral force. Both drag and lateral coefficients exhibit a dependence on non-dimensional spin parameter.
8. The different ball constructions tested produce different aerodynamic performance and, using the flight model, this is shown to have a significant effect on the flight in practical match situations.

ACKNOWLEDGEMENTS

Thanks go to the EPSRC and adidas for their sponsorship of this work. The authors are also very grateful for the many hours of work from the technicians, Rob Hunter and Keith Coulthard, who ultimately enabled the gathering of the data to be possible.

REFERENCES

- 1 **Achenbach, E.** The effects of surface roughness and tunnel blockage on the flow past spheres. *J. Fluid Mech.*, 1974, **V65**(1), 113–125.
- 2 **Achenbach, E.** Experiments on the flow past spheres at very high Reynolds numbers. *J. Fluid Mech.*, 1972, **V54**(3), 565–575.
- 3 **Achenbach, E.** Vortex shedding from spheres. *J. Fluid Mech.*, 1974, **V62**(209), 209–211.
- 4 **Rayleigh, Lord.** On the irregular flight of a tennis ball. *Mess. Math.*, 1877, **7**, 14–16.

- 5 **Davies, J. M.** The aerodynamics of golf balls. *J. Appl. Phys.*, 1949, **V20**(9), 821–828.
- 6 **Barton, N. G.** On the swing of a cricket ball in flight. *Proc. R. Soc. Lond. A, Math. Phys. Sci.*, 1982, **379**(1776), 109–131.
- 7 **Briggs, L. J.** Effect of spin and speed on the lateral deflection of a baseball; and the Magnus effect for smooth spheres. *Am. J. Phys.*, 1959, **27**, 589.
- 8 **Bearman, P. W.** and **Harvey, J. K.** Golf ball aerodynamics. *Aeronaut. Q.*, 1976, **27**, 112–122.
- 9 **Watts, R. G.** and **Ferrer, R.** The lateral force on a spinning sphere: aerodynamics of a curveball. *Am. J. Phys.*, 1987, **V55**(1), 40–44.
- 10 Available from http://fr.fifa.com/mm/document/afdeveloping/pitchequip/ims_sales_doc_05_2006_13411.pdf.
- 11 **Asai, T., Akatsuka, T., and Haake, S.** The physics of football. *Phys. World*, 1998, **11**(6), 25–27.
- 12 **Carre, M. J., Asai, T., Akatsuka, T., and Haake, S. J.** The curve kick of a football II: flight through the air. *J. Sport. Eng.*, 2002, **V5**(4), 193–200.
- 13 **Carre, M. J., Goodwill, S. R., and Haake, S. J.** Understanding the effect of seams on the aerodynamics of an association football. *Proc. IMechE, Part C: J. Mechanical Engineering Science*, 2005, **219**(C7), 657–666.
- 14 **Neilson, P. J.** and **Jones, R.** An exact method for the sphericity measurement of soccer balls. *Proc. Instn Mech. Engrs, Part B: J. Engineering Manufacture*, 2003, **217**(B5), 715–719.
- 15 **Johl, G., Passmore, M. A., and Render, P.** The design methodology and performance of an Indraft wind tunnel. *Aeronaut. J.*, 2004, **108**(1087), 465–473.
- 16 **Alam, F., Watkins, S., and Subic, A.** The aerodynamic forces on a series of tennis balls. In 15th Australasian Fluid Mechanics Conference, Sydney, Australia, December 2004.
- 17 **Watts, R. G.** and **Sawyer, E.** Aerodynamics of a knuckleball. *Am. J. Phys.*, 1975, **43**, 960–963.
- 18 **Smits, A. J.** A new aerodynamic model of a golf ball in flight. In Science & Golf II Proceedings of the World Scientific Congress of Golf, E & FN Spon, London, 1994, 340–347.
- 19 **Maccoll, J. W.** Aerodynamics of a spinning sphere. *J. R. Aeronaut. Soc.*, 1928, **32**, 777.
- 20 **Bray, K.** and **Kerwin, D. G.** Modelling the flight of a soccer ball in a direct free kick. *J. Sport. Sci.*, 2003, **21**, 75–85.
- 21 **Craig, C. M.** Judging where a ball will go: the case of curved free kicks in football. Short Communication *Naturwissenschaften*, 2006, 93:97:101 (Springer-Verlag).

APPENDIX

Notation

A	frontal area (m^2)
C_D	drag coefficient
C_{Lat}	lateral coefficient
d	ball diameter (m)
k	surface roughness (m)
r	ball radius (m)
Re	Reynolds number
Re_{crit}	critical Reynolds number
U	air speed (m/s)
ω	spin rate ($^\circ\text{s}^{-1}$)